JBUON 2016; 21(5): 1296-1306
ISSN: 1107-0625, online ISSN: 2241-6293 • www.jbuon.com
E-mail: editorial_office@jbuon.com

ORIGINAL ARTICLE

Clinical impact of SPECT-CT on bone scintigraphy in oncology: Pattern approach

Murat Tuncel, Eser Lay Ergun, Meltem Caglar Tuncali
Department of Nuclear Medicine, Hacettepe University, Faculty of Medicine, Ankara, Turkey

Summary

Purpose: *The recent addition of single photon emission computed tomography (SPECT)-CT into bone scintigraphy (BS), increased the accuracy of the test. The objective of this study was to define the main problematic scintigraphic patterns that were solved with the contribution of SPECT-CT and serve as a guide to the medical oncologist who will refer their patients to BS.*

Methods: *Two hundred and ten patients (median age 62 years, range 12-80, F/M:122/ 88) with diagnosis of cancer (breast 109;52%, prostate 63;30%, lung 15;7% and others 20;11%) were referred for BS. Subsequent SPECT-CT images (231 images from 210 patients) were obtained from the related body regions where suspicious skeletal radioactivity uptake had been observed. BS and SPECT-CT images were classified into groups according to the BS, clinical history and other imaging results in consideration with the role of SPECT-CT for more accurate diagnosis.*

Results: *SPECT-CT studies resulted in the emergence of 6 main patterns that helped improve the interpretation of the whole-body BS for more accurate diagnosis. Pattern 1: Extraskeletal uptake and/or incidental findings (14/231;6%); Pattern 2: Identification of skeletal trauma and degenerative osteoarthritic diseases (147/231;64%); Pattern 3: Benign bone tumors and reactions (12/231;5%); Pattern 4: Sclerotic-mixed type metastases (32;14%); Pattern 5: Lytic/ bone marrow metastases (12/231;5%); Pattern 6: Metabolically inactive metastases (14/231;6%).*

Conclusion*: SPECT-CT is a revolutionary technique that improved the interpretation of BS. Recognition of patterns of disease that may be resolved with SPECT-CT will help significantly to better understanding the patient's bone disease.*

Key words: *bone scintigraphy, lytic, metastases, pattern, sclerotic, SPECT-CT*

Introduction

Bone metastases play a critical role in the prognosis of patients diagnosed with cancer. Early and accurate diagnosis of these metastases are crucial to prevent complications and further disease progression. Despite advances in magnetic resonance imaging (MRI) and multi-detector computed tomography (MDCT), BS continues to play a major role in the diagnosis of bone metastases [1]. Although BS has good sensitivity for osteoblastic and mixed-type metastases, it lacks specificity. Recent addition of SPECT-CT to the standard whole-body planar images increased both the specificity and accuracy of BS. SPECT-CT improved lesion localization and characterization by providing 3D scintigraphic and anatomical images corresponding to the areas of abnormal uptake [2]. It can be difficult to distinguish between metastases and other pathological conditions such as degenerative osteoarthritic diseases which often coexist in the elderly cancer patients. Although some scintigraphic patterns could suggest the etiology, a significant number of lesions remains equivocal because of the benign uptake that could mimic malignant disease. The CT part

Correspondence to: Murat Tuncel, MD. Department of Nuclear Medicine, Faculty of Medicine, Hacettepe University, 06100 Sıhhiye, Ankara Turkey. Tel: +90 312 3051336, Fax: +90 312 3093508, E-mail:murat.tuncel@hacettepe.edu.tr, muratmtx@yahoo.com
Received : 30/01/2016; Accepted : 20/02/2016

of the study not only helps the characterization of the uptake but it also enables to detect lytic or metabolically inactive lesions that can be inherently hypo or normoactive in BS.

The aim of this study was to present different patterns of BS that SPECT-CT helped define more accurate diagnosis and to serve as a guide to the medical oncologist who will refer their patients to BS.

Methods

Between May 2013 and June 2015, 210 cancer patients (aged 12-80 years; median:62) with female/male ratio 122/88 were referred for BS for staging/restaging purposes (Table 1). Subsequent SPECT-CT images (231 images from 210 patients) were additionally obtained from the related body regions where suspicious abnormal skeletal radioactivity uptake had been observed (Table 2)

Table 1. Characteristics of 210 patients who underwent SPECT-CT

Cancer type	*N (%)*	*Indication, N (%)*	
		Staging	*Restaging*
Breast	109 (52)	40 (37)	69 (63)
Prostate	63 (30)	35 (56)	28 (44)
Lung	15 (7)	4 (27)	11 (73)
Gastrointestinal	6 (3)	0 (0)	6 (100)
Others	17 (8)	1 (6)	16 (94)
Total	210 (100)	80 (38)	130 (62)

Table 2. Body regions where the SPECT-CT images were obtained

Region of SPECT-CT	*N (%)*
Pelvic	95 (41)
Thorax	72 (31)
Abdominopelvic	32 (14)
Abdomen	14 (6)
Head and neck	9 (4)
Extremity	9 (4)
Total	231 (100)

For BS, 555-740 MBq Tc-99m-HDP (Mallincordt, USA) was injected intravenously to each patient. The patients were told to drink water for proper hydration and advised frequent voiding until the scanning time to reduce the radiation dose to the bladder wall. Three to 4 hrs after the administration of the radiopharmaceutical, each patient voided immediately prior to the scintigraphic study to eliminate bladder radioactivity for a perfect abdominopelvic image. BS was obtained by a dual-headed gamma camera (GE Infinia, USA) equipped with a high resolution, parallel-hole collimator. The imaging protocol utilized a whole-body survey (256x1024 matrix, scan speed: 10cm/min).

Additional SPECT-CT images from suspicious areas were obtained on a on a dual-headed gamma camera equipped with a low-power X-ray system (Millenium, VG & Hawkeye™; GE Medical Systems, Milwaukee, WI). SPECT acquisition was performed with high-resolution low-energy collimators, with matrix size of 128 x 128, 3° angle steps and 25 sec per frame. Transmission SPECT-CT data were acquired over 360° during 14 sec for each transaxial slice with a thickness of 5 mm.

BS and SPECT-CT images were then interpreted on a Xeleris Workstation (GE, USA). The scintigraphic results were correlated with the patients' clinical history and other avalaible imaging study results such as direct X-ray films or Magnetic Resonance Imaging (MRI). SPECT-CT findings were classified into groups according to the BS, clinical history and other imaging results in consideration with the role of SPECT-CT for more accurate diagnosis.

Results

SPECT-CT studies resulted in the identification of 6 main patterns that helped improve the interpretation of the whole-body BS for more accurate diagnosis.

Pattern 1: Extraskeletal uptake and/or incidental findings

This group consisted of 14 patients and 14/231 (6%) of all SPECT-CTs. Planar BS showed abnormal Tc-99m HDP uptakes in bone regions. SPECT-CT verified that there was no metastatic bone disease in these regions and identified that the causes of abnormal BS uptakes were extraskeletal obscuring the underlying bony structures. SPECT-CT also detected additional extraskeletal findings. In this group, SPECT-CT was complementary for the BS in the exclusion of bone metastases and detecting additional/incidental findings which were important for the further management of patients. The most common examples in this group were patients after cystectomy and urinary diversion obscuring the pelvic structures (Figure 1), calcificied stones in the urinary system showing increased radiotracer uptake (Figure 2), heterotopic ossifications, ectopic kidney and soft tissue metastases (Table 3).

Pattern 2: Identification of skeletal trauma and degenerative osteoarthritic diseases in patients with cancer

This is the most common application of SPECT-CT. This group consisted of 135 patients and 147/231 (64%) of all SPECT-CTs. SPECT-CT

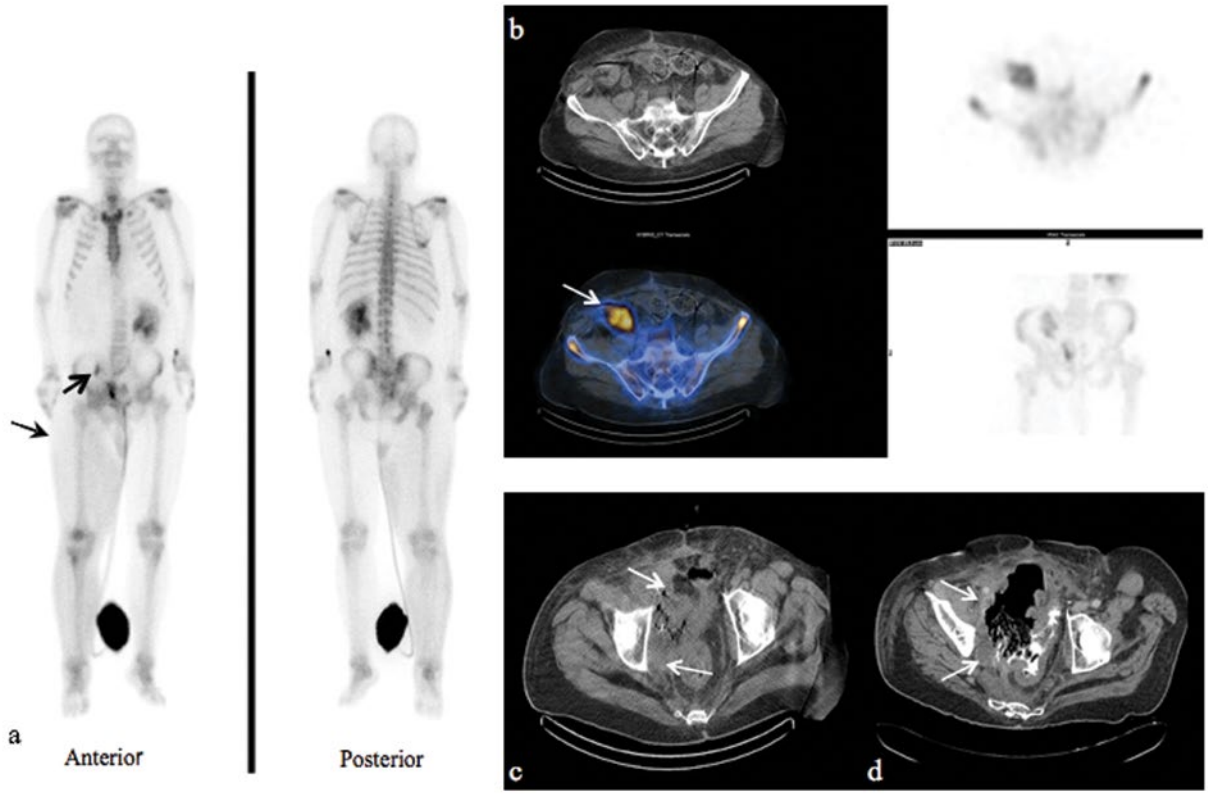

Figure 1. Whole-body BS **(a)** shows increased uptake on the right sacroiliac region and diffuse right lower extremity soft-tissue uptake (black arrows) in a patient with bladder cancer. SPECT-CT images **(b)** indicate the uptake in sacroilliac region is located at the Indiana pouch (arrow). Low dose CT of SPECT-CT **(c)** and diagnostic CT **(d)** display locally invasive recurrence of the disease compressing the adjacent structures and leading to edema in right lower extremity (arrows).

identified that the abnormal suspicious uptakes on BS were due to skeletal trauma and/or degenerative osteoarthritic diseases other than metastases. The common etiologies in this group were vertebra end-plate degenerative changes/osteophytes (Figure 3), facet artropathy, enthesopathies, benign fractures etc. (Table 3).

Pattern 3: Benign bone tumors and reactions

This group included 12 patients and 12/231 (5%) of all SPECT-CTs. BS revealed increased uptake in the bone structures that were suspicious for metastases. SPECT-CT excluded metastases and characterized the bone accumulations as benign bone tumors or bone reactions secondary to a malignant processes like hyperostosis frontalis interna (Figure 4), hypertrophic osteoartropathy (Figure 5), Paget's, disease, fibrous dysplasia, exostosis etc (Table 3).

Pattern 4: Sclerotic-mixed type metastases

This group consisted of 28 patients and

Table 3. Etiology of uptakes defined by SPECT-CT patterns 1, 2 and 3

	Pattern 1, N (%)	*Pattern 2, N (%)*	*Pattern 3, N (%)*
	Calcific stones in urinary system 4 (29)	Vertebra end-plate degeneration or osteophytes 71 (48)	Hyperostosis frontalis interna 5(41)
	Cystectomy and urinary diversion 3 (21.5)	Facet artropathy 32 (22)	Hypertrophic osteoartropathy 2(17)
	Heterotrophic ossification after trauma or surgery 3 (21.5)	Benign fractures 24 (16)	Paget 2(17)
	Ectopic kidney 2 (14)	Enthesopathies 16 (11)	Fibrous dysplasia 2(17)
	Soft tissue metastases 2 (14)	Sacroilleitis 4 (3)	Exostosis 1(8)
Pattern, total	14 (100)	147 (100)	12 (100)
Total, N (%): 231 (100)	14 (6)	147 (64)	12 (5)

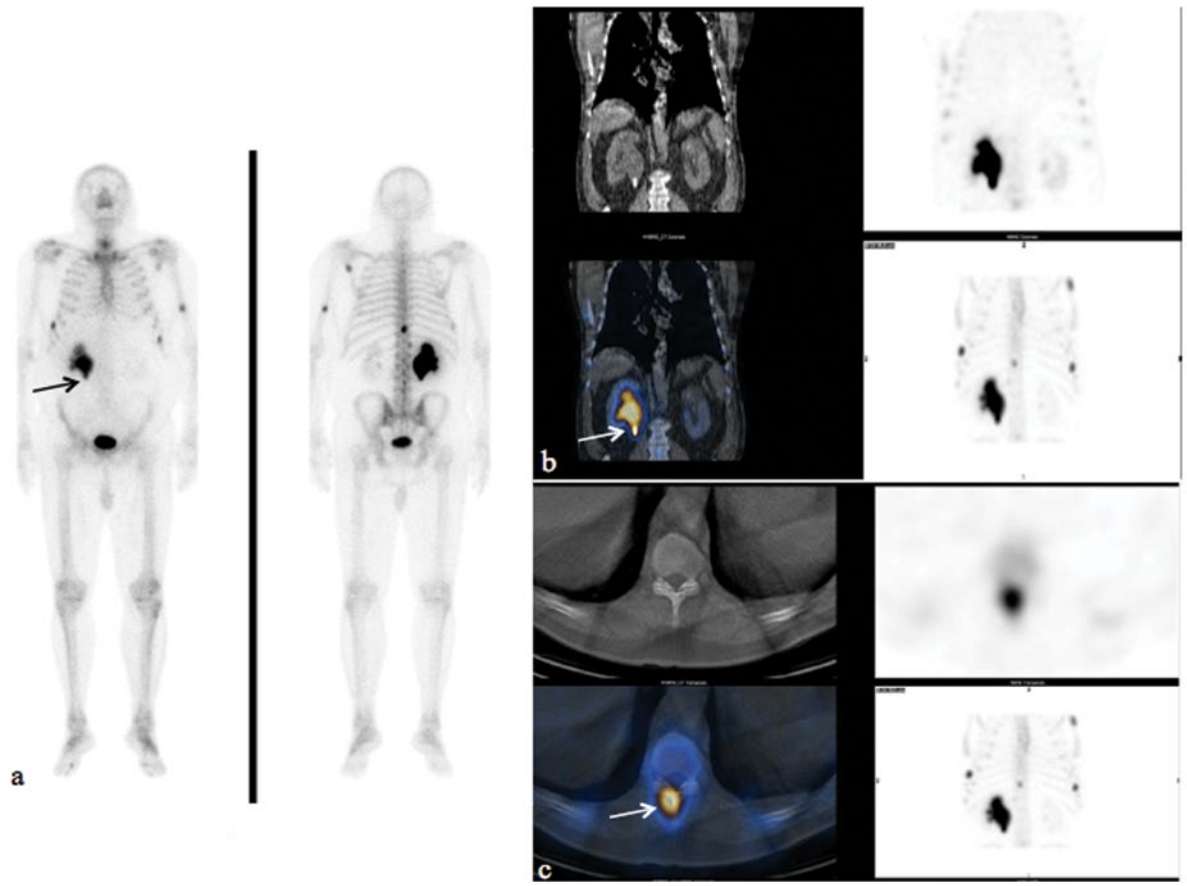

Figure 2. Whole-body BS shows increased Tc-99m HDP uptake on T11 vertebra, the 8th right and left ribs, left scapula, left humerus and right acetabulum. Arrow shows the significant retention of radiotracer in the right renal pelvis **(a):** SPECT-CT images **(b)** indicate a proximal ureteral stone causing obstruction and dilatation of the right renal pelvis and **(c)** sclerotic bone metastasis on T11 vertebra spinous process (arrowhead in CT, arrow in fusion images and arrows in cross-sectional and maximum intensity projection (MIP) SPECT images of SPECT-CT respectively).

Table 4. Etiology of uptakes defined by different SPECT-CT pattern 4,5 and 6

	Pattern 4, N (%)	*Pattern 5, N (%)*	*Pattern 6, N (%)*
	Breast cancer 16 (50)	Breast cancer 5 (42)	Breast cancer 5 (36)
	Prostate cancer 8 (25)	Sarcoma 2 (17)	Prostate cancer 3 (21)
	Lung cancer 4 (13)	Thyroid cancer 2 (17)	Neuroendocrine tumor 3 (21)
	Colon cancer 2 (6)	Lung cancer 1 (8)	Colon cancer 2 (14)
	Neuroendocrine tumor 2(6)	Colon cancer 1 (8)	Cervix cancer 1(8)
		Renal cancer 1 (8)	
Pattern, total	32 (100)	12 (100)	14 (100)
Total, N (%): 231 (100)	32 (14)	12 (5)	14 (6)

32/231 (14%) of all SPECT-CTs. BS revelead increased uptake in the bone structures that were suspicious for metastases. SPECT-CT confirmed the metastases and classified the lesions as sclerotic or mixed type. In 7 patients, SPECT-CT also showed a total of 14 additional and small metastases (median size 6.5±3 cm ;range 4-12) which were not clearly visible on whole-body planar BS (Figure 6). This group included sclerotic-mixed type metastases of the breast, prostate, lung, colon cancer etc (Table 4).

Pattern 5: Lytic/bone marrow metastases

This group included 12 patients and 12/231 (5%) of all SPECT-CTs. SPECT-CT helped detect lytic/ bone marrow metastases with secondary uptake due to weakened bone or without any increased uptake on BS (Figure 7). This group consisted of patients with malignancies that could make lytic metastases like breast cancer, sarcoma, lung cancer, renal cancer, colon cancer and thyroid cancer (Table 4).

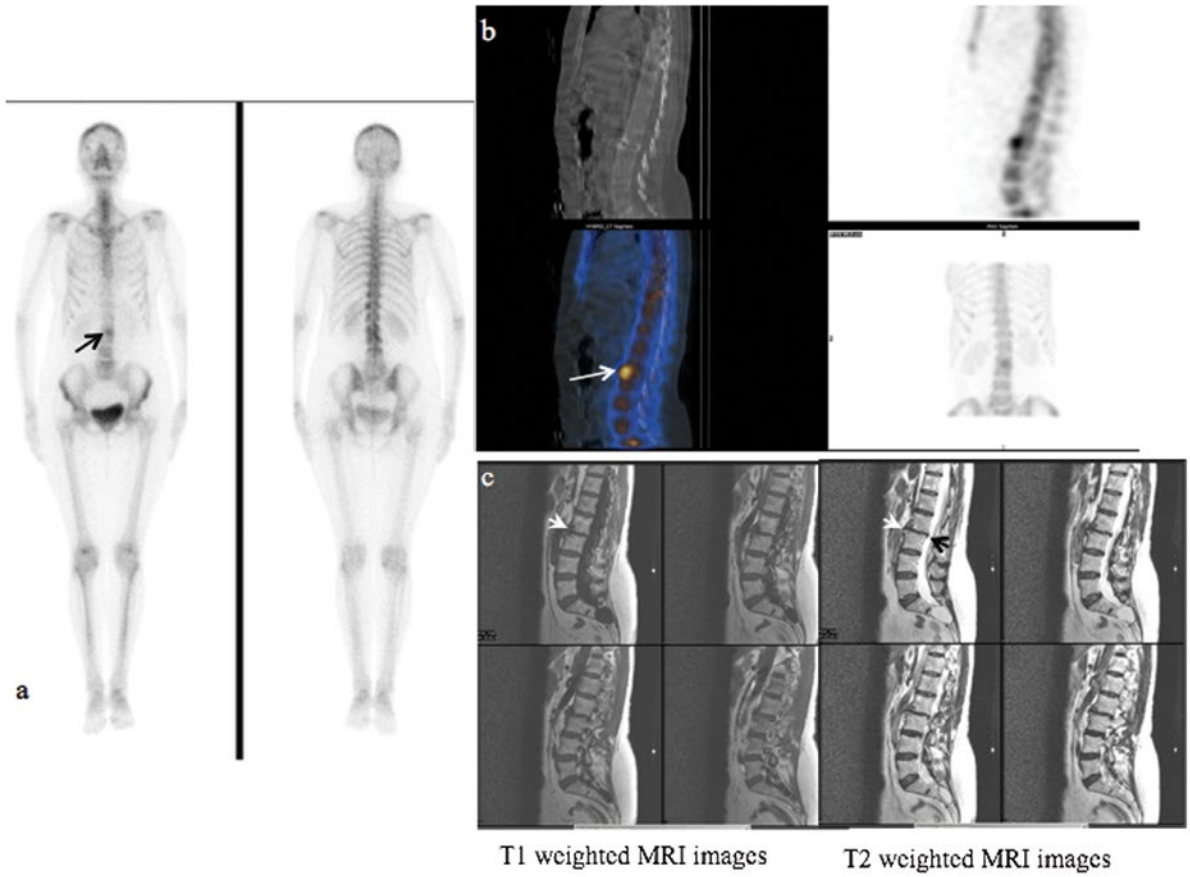

Figure 3. Whole-body planar BS images **(a)** show increased uptake in the L3 vertebra (arrow). SPECT-CT **(b)** indicates sclerosis at the superior endplates of L2 and L3 vertebrae and accompanying osteophytes (arrows in CT and fusion images of SPECT-CT and arrows in sagittal and MIP SPECT image). Corresponding MRI images **(c)** confirm the sclerosis as seen hypointense on both T1 and T2 weighted images which is compatible with Modic type 3 changes (arrowhead). Arrowhead shows a posterior protrusion of the intervertebral disc which is commonly accompanied with endplate sclerosis as seen in Figure 3b.

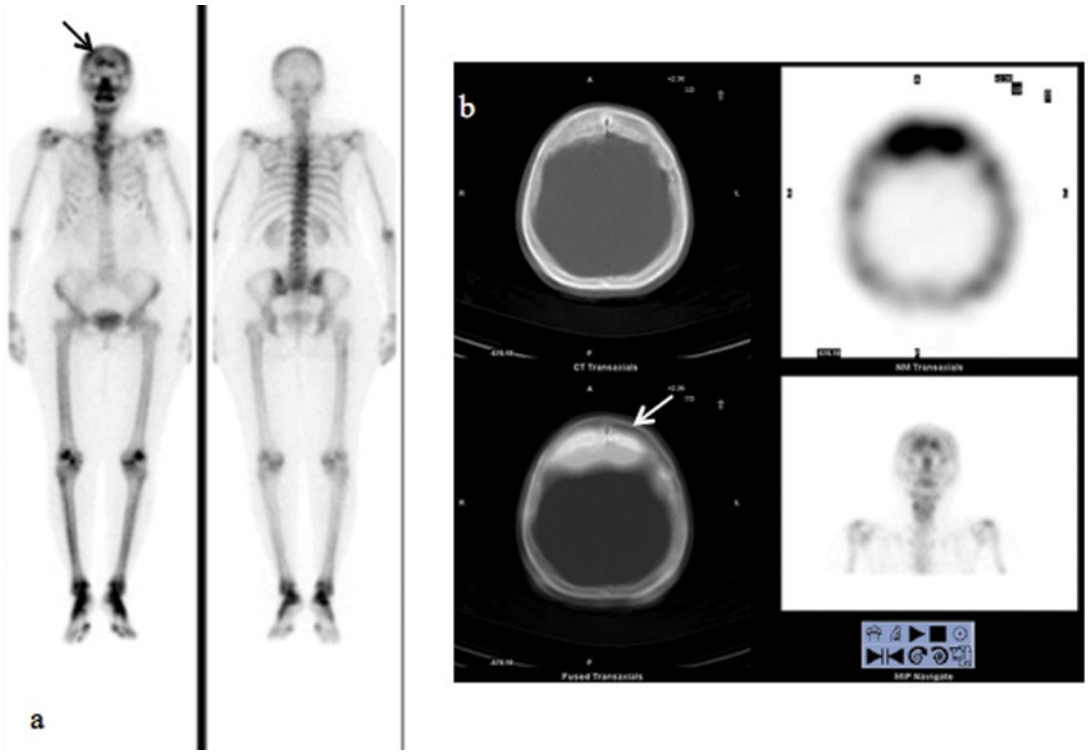

Figure 4. Whole-body BS of a patient with breast cancer **(a)** indicates suspicious irregular increased uptake in the frontal bone arrow. SPECT-CT images **(b)** display increased uptake in the frontal bone which shows symmetric thickening and benign overgrowth of the inner table compatible with 'hyperostosis frontalis interna' (arrows in CT and fusion images and black arrows in axial and MIP SPECT images of SPECT-CT, respectively).

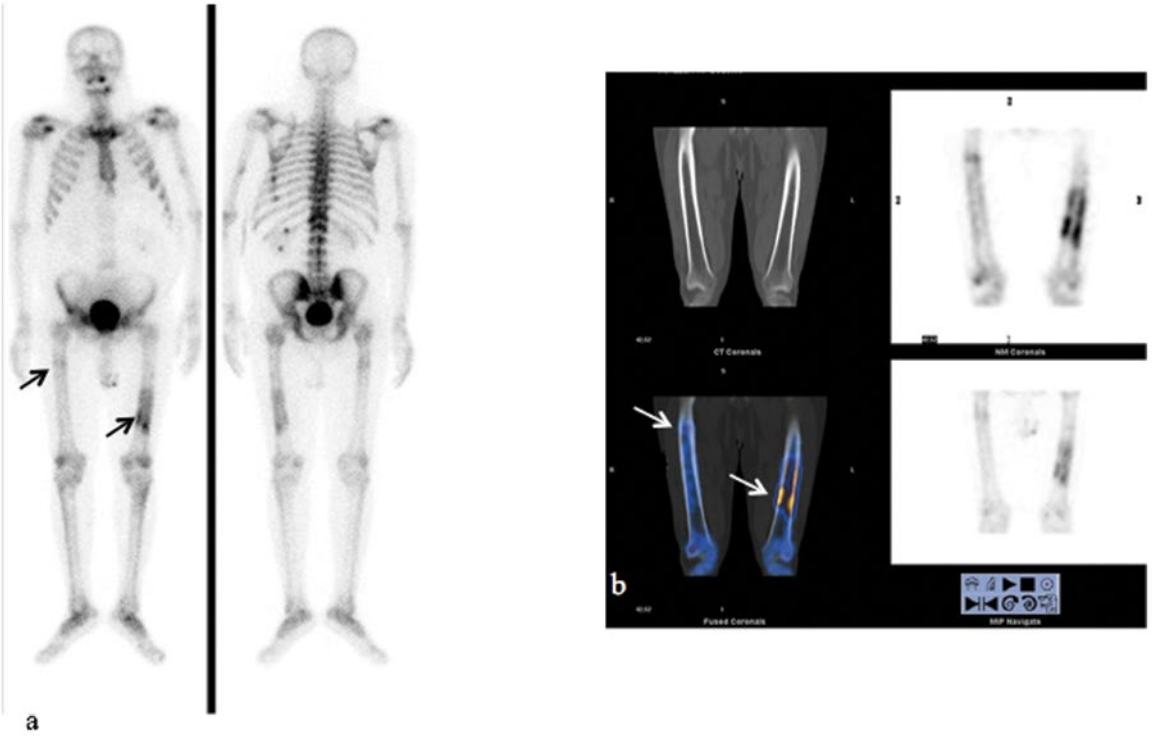

Figure 5. Whole-body BS of a patient with lung cancer **(a)**: Arrows show increased asymmetric uptake in both femurs. SPECT-CT images **(b)** indicate cortical distribution of the radioactivity uptake in both femurs without destruction on CT images which is compatible with hypertrophic osteoartropathy (arrows at fusion and arrows at SPECT images of SPECT-CT).

Pattern 6: Metabolically inactive metastases

This group included 12 patients and 14/231 (6%) of all SPECT-CTs. The patients of this group received therapy after the diagnosis of bone metastases and referred to BS for re-staging. SPECT-CT identified the sclerotic metastases without significant uptake secondary to effective therapy (Figure 8). These patients had breast cancer, prostate cancer, colon cancer, neuroendocrine tumor and cervix cancer.

Discussion

BS is used as a routine screening test for suspected bone metastases because of its high sensitivity, availability and low cost. But, unfortunately its specificity is low. SPECT-CT is a revolutionary technique that tremendously increased the accuracy and specificity of the scintigraphic studies by providing accurate localization and characterisation of equivocal lesions on scintigraphic studies such as In-111 octreotide scintigraphy, I-123 MIBG scintigraphy and bone scintigraphy as well [3].

In the present study, we classified the BS patterns in cancer patients into 6 main groups according to SPECT-CT findings to obtain a more accurate and systematic design for the interpretation of BS. According to our results in cancer patients, there were 6 distinct patterns that could be recognized with SPECT-CT.

The first pattern was the extraskeletal and incidental findings. In this group of patients SPECT-CT helped characterize the extraskeletal uptake of the tracer and additional/incidental findings. There are several extraskeletal uptake sites of the bone tracer [4,5]. The reason for the extraskeletal uptake may be due to the excretion of the tracer to the urinary system /small amount to bowel or adsorpition of tracer into extraskeletal bone forming/calcification processes like heterotopic ossification or tumors like neuroblastoma. As seen in our cases, the urinary excretion of the tracer to the Indiana pouch (Figure 1) or excretion via ectopic kidney could lead to a diagnostic problem, especially when superexposed to bony structures. It can be argued that the uptake sites can also be explained by SPECT imaging. However, SPECT could only show that the uptake site was in the soft tissue but the exact structure that caused this uptake is unpredictable. The CT portion of the study would be very useful, especially when the clinical history and correlative imaging are lacking. The CT portion of the study could also change the management and explain the etiolo-

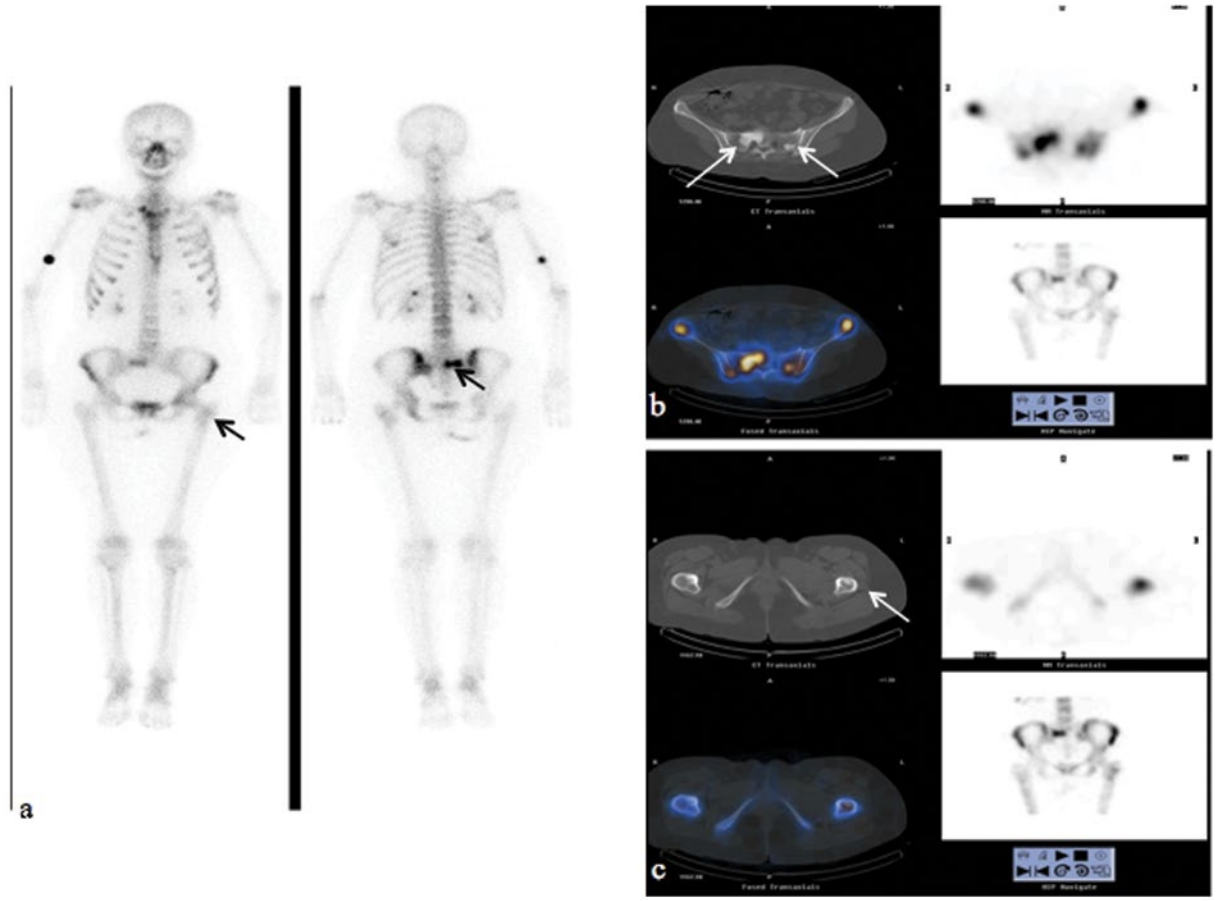

Figure 6. Whole-body BS images of a patient with breast cancer **(a)** show increased uptake in the right sacrum and slight uptake on the left proximal femur (arrows**)**. SPECT-CT images reveal diffuse sclerotic lesions corresponding to the increased uptake in planar imaging and additional smaller metastatic sclerotic lesions in the left sacrum **(b)** and left femur **(c)** (arrows in CT and fusion images and arrowheads at axial and MIP SPECT images of SPECT-CT, respectively) which are not clearly seen with planar imaging.

gy of extraskeletal uptake as in Figure 2 in which increased radioactivity retention in the upper collecting system of the kidney was explained by obstructing ureteral stone and in Figure 1 in which the CT portion of SPECT-CT detected local recurrence that explained the etiology of the increased soft tissue radiotracer uptake secondary to right extremity edema. These cases show the superiority of SPECT-CT over SPECT on the basis of detecting abnomalities that can not be observed by SPECT alone.

The second pattern of SPECT-CT was the identification of skeletal trauma and degenerative osteoarthritic changes in patients with cancer. This pattern of patients was among the most common ones that are faced in the clinical routine and also in our study, Degenerative bony changes were common among patients with cancer due to advanced age. Especially in osteoarthritis the scintigraphic images may mimic bone metastases. Bone SPECT-CT may help in the identification of these mimicking conditions by identification of the exact localization of the uptake and degenerative osteoartritic changes like endplate sclerosis (Figure 3), schmorl nodules, fracture lines. SPECT-CT was approved as an useful method for this purpose when compared to planar imaging and SPECT [6]. Helyar et al. evaluated 50 lesions on planar BS in 40 patients. On reporting the planar study and SPECT scans, the authors rated 61% of lesions as equivocal. SPECT-CT scans decreased the equivocal lesions to 8%, 24% of these lesions were rated as malignant and 68% as benign. SPECT-CT also increased the inter-reviewer agreement. Weighted kappa scores for inter-reviewer agreement were 0.43 for bone scintigraphy, 0.56 for SPECT and 0.87 for SPECT/CT with $p<0.0001$ [7]. Similarly, our study found 50% decrease in equivocal lesions by the introduction of SPECT-CT [8]. Most of the equivocal uptakes were turned to benign uptake mostly because of degenerative osteoarthritic disease. The problem with the planar BS

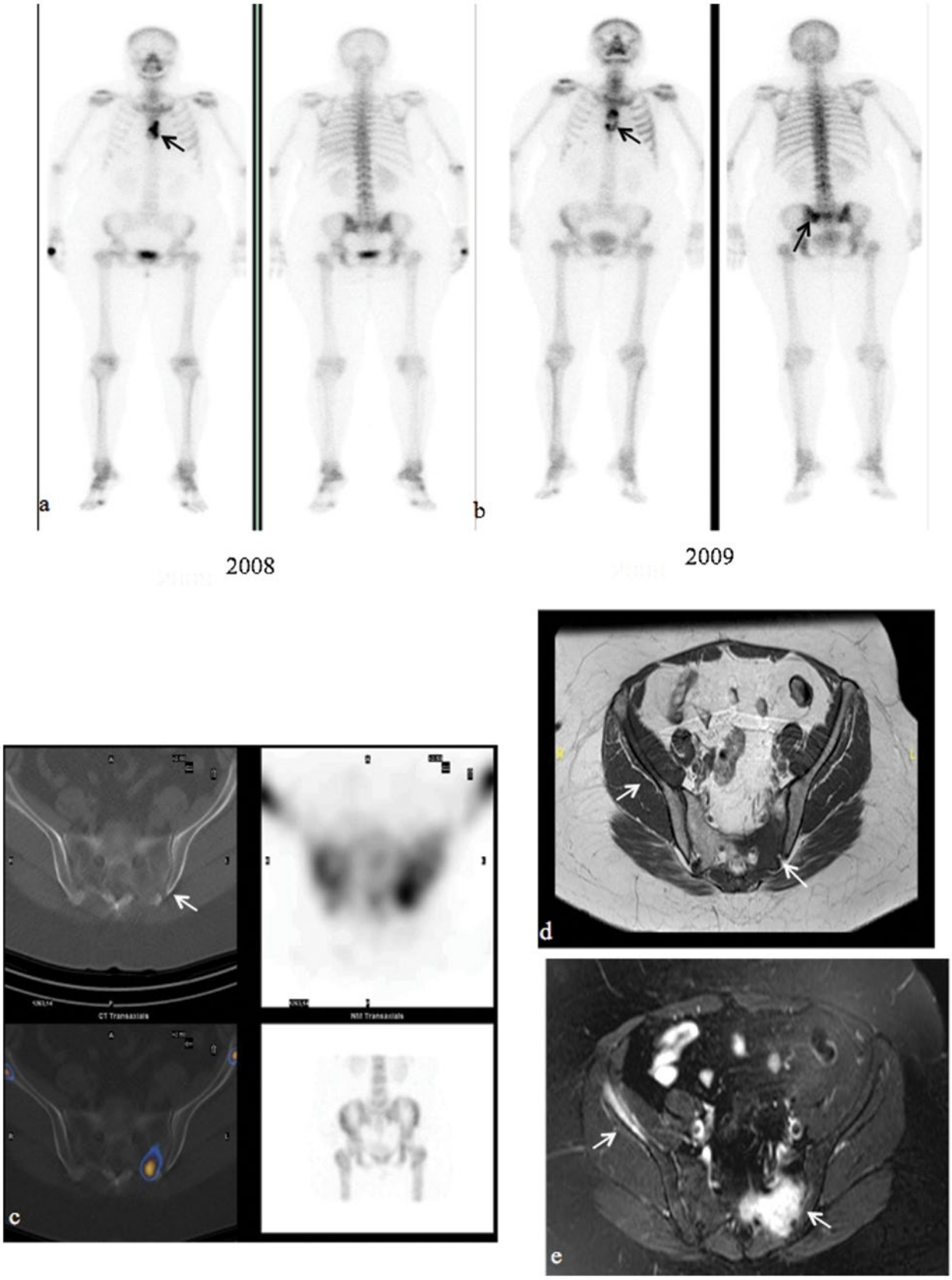

Figure 7. Whole-body BS images **(a)** from 2008 revealed increased uptake in the sternum (arrow) which was slightly increased in extent and showed a hypoactive area in the middle at 2009 **(b)** when compared to previous study **(a)**. Additionally, whole-body images showed a slightly increased uptake in the sacrum (arrowhead) **(b)**. SPECT-CT images **(c)** revealed increased uptake in a small fracture line at sacrum which is perpendicular to the classic insufficency fracture (arrows at CT and fusion images and arrows at axial and MIP SPECT images of SPECT-CT, respectively). T1 weighted MRI images **(d)** showed hypointense destructive metastases in the left part of the sacrum and right illiac bone which were hyperintense in T2 weighted STIR images (arrows) **(e)**.

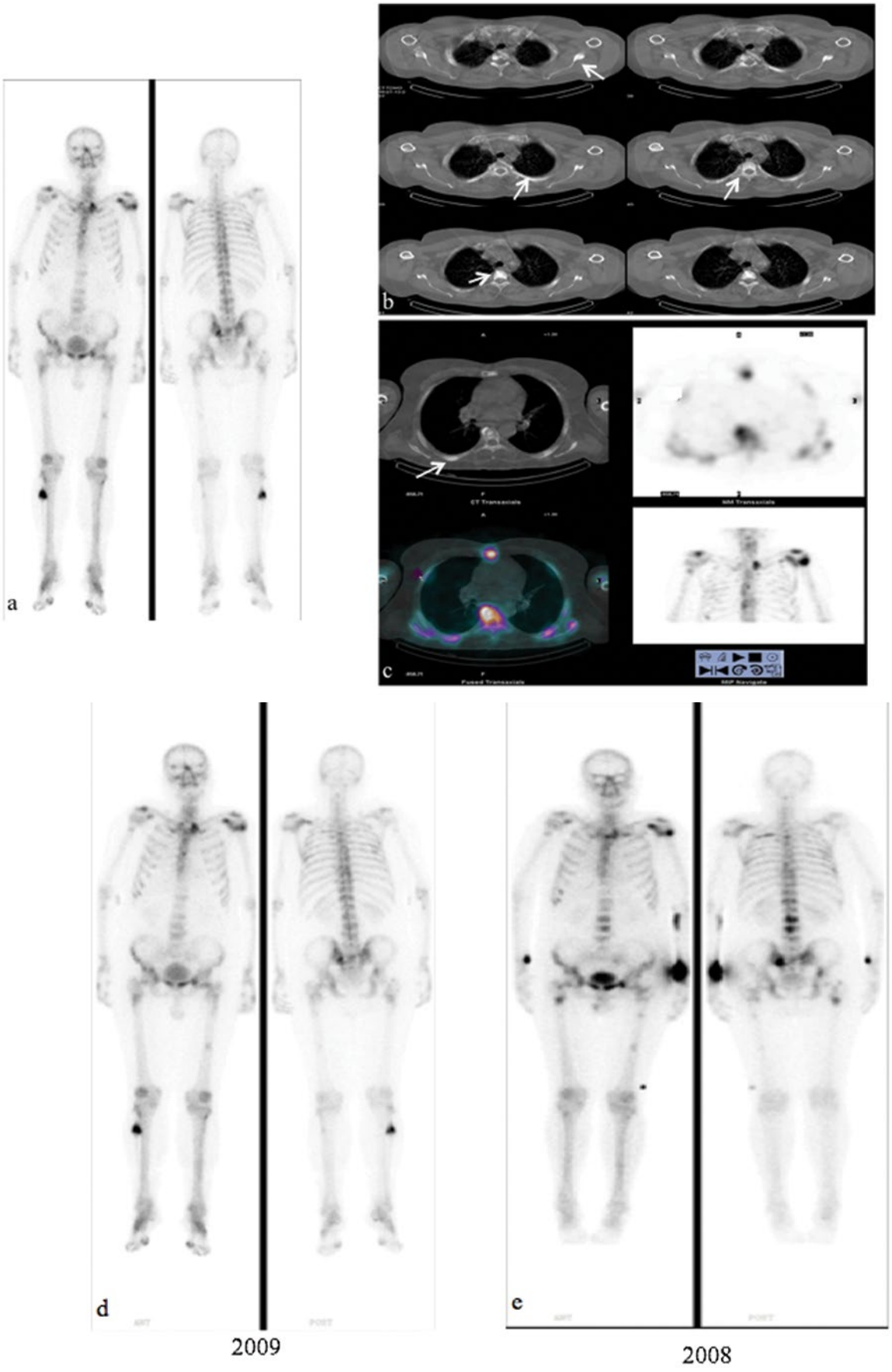

Figure 8. Whole-body BS images from 2009 **(a)** showed metastatic uptake in both femurs and the right tibia (arrows), but also suspicious uptake in pelvic bones and nearly normal in the other parts of the body. SPECT-CT images from the chest **(b,c)** showed extensive sclerotic metastases in the sternum, ribs and scapulas (arrows in the CT part of SPECT-CT images), which showed mild or normal uptake (arrows in axial and MIP SPECT images). The patient's previous BS from 2008 **(d)** showed previously metabolically more active bone metastases (arrowheads).

mainly comes from the 2D nature of the images which cannot exactly define the localization of the lesion, a point that is crucial for characterization of the disease. Although SPECT could provide better localization, it is still insufficient for exact diagnosis [6-8]. Ndlovu et al. compared SPECT and SPECT-CT in a group of patients suffering from prostate or breast cancer. SPECT/CT resulted in a significant reduction in the proportion of patients (from 48 to 14%, p=0.0015) and lesions (from 31 to 9%, p< 0.0001) with equivocal SPECT findings. The overall accuracy of SPECT/CT was significantly higher than SPECT alone on both a patient-wise (52–79%, p=0.0026) and lesion-wise basis (67–92%, p<0.0001) [9]. The detection of benign changes like fracture line, osteophytes etc. without metastatic sclerotic or mixed lesion with the CT portion increased the confidence in image interpretation.

The third pattern was the benign bone tumor and bony reactions. Although uncommon, there are patients that have benign bone lesions (exostosis, fibrous dysplasia etc) or bony reactions secondary to malignant primary disease (hypertrophic osteoartropathy etc). The problem with these disease conditions is that they may lead to increased uptake that can be misinterpreted as metastatic disease. SPECT-CT help the diagnosis by identifying the exact localization and morphology of the uptake which helps in the differential diagnosis as Figure 5 shows, although the uptake in the planar images looked more diffuse and asymmetric in both femurs which is mostly compatible with the diagnosis of bone metastases. SPECT-CT showed cortical distribution of the bone tracer without bone destruction which is typical for hypertropic pulmonary osteoarthropathy as also reported by Russo et al [10]. The CT portion of the study also identified critical image findings to reach a final diagnosis like sclerotic lesion in ground glass density without extraosseous extension, which is typical for fibrous dysplasia in fronto-nasal region and typical exophytic bone formation in exostosis of the pelvic bones. There are also other entities in which the CT portion of SPECT-CT could help in the diffferential diagnosis like osteoid osteoma, hyperostosis frontalis interna (Figure 4), Paget's disease etc [11] which could be included in the third pattern.

The fourth pattern was the sclerotic or mixed type metastases. In this group of patients SPECT-CT confirmed the uptake in the scintigraphy by showing the corresponding sclerotic-mixed type of metastatic lesions and better localized the lesions as in vertebral corpus or pedicle etc. SPECT-CT also identified additional lesions which might be missed with planar and SPECT images. The significance of additional lesions was discussable when the patient received systemic therapy. When the patient was scheduled for regional therapy, like radiotherapy or surgical removal of a solitary metastasis, the exact extent of metastatic disease becomes more important. Additional small lesions missed by planar BS but detected by SPECT-CT may change the ratiation field or avoid morbid surgery by identifying more extensive disease. Radiation oncologists should not decide on their therapy planning by the interpretation of the planar BS images solely because SPECT-CT could play a great role in this respect. Additionally, if the efficacy of systemic therapy will be followed by BS, the presence of these additional lesions should be known in order not to misinterpret the scintigraphic findings as diseases progression. In this group of patients the CT portion of SPECT-CT also identified if the metastatic lesion is sclerotic or mixed type and this knowledge has a prognostic value. It has been shown that patients with mixed type metastases had a worse prognosis [11,12].

The fifth pattern included lytic or bone marrow metastases. BS in these patients were negative in the metastatic lesion but show increased uptake due to fractures or bone reactions secondary to lytic metastases. SPECT-CT showed lytic metastatic lesions in the CT part of the technique and revealed fractures of weakened bone (Figure 7). BS is not the preferred imaging modality in the detection of lytic metastases. Imaging modalities like FDG-PET and whole-body MRI are the modalities of choice in this particular group of patients [12,13]. This finding was reported by many authors [14]. Cook et al. have compared FDG-PET and planar BS in 23 breast cancer patients with osteoblastic and osteolytic bone metastases. Although overall more metastases were detected by FDG-PET, BS was more sensitive in a subgroup of patients with osteoblastic disease [15]. Nakai et al. reported a sensitivity of 100% for the detection of lytic skeletal metastases with FDG-PET vs 70% for BS, compared with 56% and 100%, respectively, for sclerotic lesions [16]. Uematsu et al. have compared FDG-PET and BS-SPECT in 15 breast cancer patients with known bone metastases, who had 143 osteoblastic and 20 osteolytic lesions. The sensitivity of SPECT was 92% for sclerotic (including also mixed lesions) and 35% for osteolytic lesions, compared with sensitivities of 6% and 90%, respectively, for FDG-PET [17]. This finding may change with the introduction of SPECT-CT. The question is from which areas the nuclear medicine physcian should obtain SPECT-

CT images while the BS is negative. Our suggestion would be the areas that cause pain and high prevalance of metastases but this must be proved in prospective studies.

The sixth pattern was with patients whose BS were acquired during their follow-up. SPECT-CT identified sclerotic lesions which show normal or near-normal uptake. These are the lesions that have lost their metabolic activity after radiation therapy or chemo/hormonotherapy. The finding is well demonstated on patients with prostate cancer [18] and SPECT-CT provides better understanding of the disease.

In the fifth and the sixth pattern, SPECT-CT not only helped in the differential diagnosis but also detected disease conditions which are undetectable with scintigraphy alone, like metabolically inactive sclerotic metastases and lytic lesions which do not lead to an osteoblastic reaction.

The radiation burden from the CT portion of the study is another important issue to be discussed. SPECT-CT that we used was proved to give very low radiation doses. The average effective doses from CT scans acquired using the Hawkeye were 0.9 mSv for a chest scan, 1.5 mSv for an abdomen-pelvis scan, and 0.1 mSv for a head scan, all significantly lower than doses resulting from diagnostic CT scans (3,7,1 and 1,5 mSv, respectively) [19], and BS itself (5,9 mSv for an adult patient) [20].

Conclusion

SPECT-CT is a revolutionary technique that improved the interpretation of bone scintigraphy. Recognition of patterns of disease that may be faced with SPECT-CT will significantly help in better understanding of the patient's disease and lead to a more accurate answer to the clinical question.

Conflict of interests

The authors declare no confict of interests.

References

1. Söderlund V. Radiological diagnosis of skeletal metastases. Eur Radiol 1996;6:587-595.
2. Mariani G, Bruselli L, Kuwert T et al. A review on the clinical uses of SPECT/CT. Eur J Nucl Med Mol Imaging 2010;37:1959-1985.
3. Buck AK, Nekolla SG, Ziegler SI, Drzezga A. SPECT/CT. J Nucl Med 2009;49:1305-1319.
4. Tuncel M, Erbas B, Mahmoudian B. Gamut:soft tissue uptake of bone radiopharmaceuticals. Semin Nucl Med 2003;33:334-337.
5. Ergün EL, Kiratli PO, Günay EC, Erbaş B. A report on the incidence of intestinal 99mTc-methylene diphosphonate uptake of bone scans and a review of the literature. Nucl Med Commun 2006;27:877-885.
6. Gnanasegaran G, Barwick T, Adamson K, Mohan H, Sharp D, Fogelman I. Multislice SPECT/CT in benign and malignant bone disease: when the ordinary turns into the extraordinary. Semin Nucl Med 2009;39:431-442.
7. Helyar V, Mohan HK, Barwick T et al. The added value of multislice SPECT/CT in patients with equivocal bony metastasis from carcinoma of the prostate. Eur J Nucl Med Mol Imaging 2010;37:706-713.
8. Caglar M, Velipasaoglu Z, Tuncel M. SPECT-CT offers high diagnostic accuracy when findings on planar bone scintigraphy are inconclusive. Eur J Nucl Med Mol Imaging 2010;37 (Suppl 2):S198-S311.
9. Ndlovu X, George R, Ellmann A, Warwick J. Should SPECT-CT replace SPECT for the evaluation of equivocal bone scan lesions in patients with underlying malignancies? Nucl Med Commun 2010;31:659-665.
10. Russo RR, Lee A, Mansberg R, Emmett L. Hypertrophic pulmonary osteoarthropathy demonstrated on SPECT/CT. Clin Nucl Med 2009;34:628-631.
11. Nadel HR. Bone scan update. Semin Nucl Med 2007;37:332-339.
12. Pahade J, Sekhar A, Shetty SK. Imaging of malignant skeletal tumors. Cancer Treat Res 2008;143:367-422.
13. Fogelman I, Cook G, Israel O, Van der Wall H. Positron emission tomography and bone metastases. Semin Nucl Med 2005;35:135-142.
14. Ben-Haim S, Israel O. Breast cancer: role of SPECT and PET in imaging bone metastases. Semin Nucl Med 2009;39:408-415.
15. Cook GJ, Houston S, Rubens R, Maisey MN, Fogelman I. Detection of bone metastases in breast cancer by 18FDG PET: Differing metabolic activity in osteoblastic and osteolytic lesions. J Clin Oncol 1998;16:3375-3379.
16. Nakai T, Okuyama C, Kubota T et al. Pitfalls of FDG-PET for the diagnosis of osteoblastic skeletal metastases in patients with breast cancer. Eur J Nucl Med Mol Imaging 2005;32:1253-1258.
17. Uematsu T, Yuen S, Yukisawa S et al. Comparison of FDG PET and SPECT for detection of bone metastases in breast cancer. AJR 2005;184:1266-1273.
18. Scher H. Prostate carcinoma: defining therapeutic objectives and improving overall outcomes. Cancer (Suppl 3) 2003;97:758-771.
19. Sawyer LJ, Starritt HC, Hiscock SC, Evans MJ. Effective doses to patients from CT acquisitions on the GE Infinia Hawkeye: a comparison of calculation methods. Nucl Med Commun 2008;29:144-149.
20. Donohoe KJ, Henkin RE, Royal HD et al. Procedure guideline for bone scintigraphy: 1.0. Society of Nuclear Medicine. J Nucl Med 1996;37:1903-1906.